Coverage Optimization for UAV-Aided Internet of Things with Partial Channel Knowledge

Xuanxuan Wang[1,2], Wei Feng[1,2], Yunfei Chen[3], Ning Ge[1,2]

1. Beijing National Research Center for Information Science and Technology (BNRist), Tsinghua University, Beijing, China
2. Department of Electronic Engineering, Tsinghua University, Beijing, China
3. School of Engineering, University of Warwick, Coventry, CV4 7AL, UK

Abstract: Due to the high maneuverability of unmanned aerial vehicles (UAVs), they have been widely deployed to boost the performance of Internet of Things (IoT). In this paper, to promote the coverage performance of UAV-aided IoT communications, we maximize the minimum average rate of the IoT devices by jointly optimizing the resource allocation strategy and the UAV altitude. Particularly, to depict the practical propagation environment, we take the composite channel model including both the small-scale and the large-scale channel fading into account. Due to the difficulty in acquiring the random small-scale channel fading, we assume that only the large-scale channel sate information (CSI) is available. On this basis, we formulate an optimization problem, which is not convex and challenging to solve. Then, an efficient iterative algorithm is proposed using block coordinate descent and successive convex optimization tools. Finally, simulation results are presented to demonstrate the significant performance gain of the proposed scheme over existing ones.

Keywords: block coordinate descent, coverage optimization, Internet of Things (IoT), unmanned aerial vehicles (UAVs)

1 Introduction

Internet of Things (IoT) is one of the crucial applications of the ongoing fifth generation (5G) system [1-6]. It significantly improves the quality of our daily life by connecting a large number of devices. Generally, IoT devices are energy-limited [7,8], such as remote sensors, they are hardly able to transmit over a long distance and difficult to be served by the IoT server.

Nowadays, utilizing unmanned aerial vehicles (UAVs) as an aerial base station (BS) to serve the ground IoT devices has attracted more and more interest [9-16]. By leveraging the high mobility of UAVs, it is able to move sufficiently close to the IoT devices to collect the data from them, and then transmit it to the central Processor. Thus, the UAV-aided IoT communication system becomes beneficial for coverage expansion and overhead reduction of the IoT networks. In addition, UAVs are usually cost-effective [17-19]. They are quite suitable for on-demand emergency mission in the IoT communications. Furthermore, the high maneuverability of UAVs could offer an additional degree of freedom to dynamically adjust the UAV altitude to best suit the queries from the IoT devices.

In the existing literatures, some researchers focused on maximizing the sum rate performance of a UAV-aided communication system [20-22]. In [20], the authors studied the throughput maximization problem subject to the constraints on the source/relay transmit power, the relay trajectory, practical mobility and the information-causality. The authors in [21] maximized the approximate ergodic sum rate via dynamically adjusting the UAV heading. In [22], the authors adopted the UAV as an aerial BS and analyzed both the UAV power and its sum-rate capacity gain. Some other works focused on the energy efficiency maximization to enhance the system performance [23,24]. For example, the authors in [23] aimed to maximize the energy efficiency of UAV communications. By jointly optimizing the wake-up schedule of sensors and the trajectory of UAV, the authors in [24] minimized the maximum energy consumption of all the sensors to make sure the data can be reliably collected from the sensors. In addition, to analyze the outage probability of the system is also of vital importance for the performance enhancement. By analyzing the severe limitation imposed by a fixed-wing unmanned aircraft on the circular flight operation, the authors in [25] proposed a variable-rate relaying approach to optimize the achievable performance in terms of outage probability and information rate. In [26], the authors derived the analytical expressions for the optimal UAV to minimize the outage probability of air-to-ground links. The authors in [27] analytically obtained and calculated the outage performance for the non-orthogonal multiple access based unmanned aerial vehicles satellite networks. In [28], the authors studied the optimum placement of UAV as an aerial BS by deriving the overall outage probability and the overall bit error rate (BER).

Although these works have provided very useful guidance on optimizing the UAV-enabled communication system, they might not be directly used for the IoT environment, where coverage performance is a more important issue to be considered. In the IoT communication system, to support the on-demand mission, such as disaster relief operations, surveillance, forest fire monitoring and so on, a large amount of IoT devices are randomly scattered over a wide area for their different targets. Accordingly, how to enlarge the coverage of IoT communications is quite vital.

In fact, the coverage optimization problem of the UAV-aided communication system has been partially studied. For example, in [29], the authors maximized the minimum throughput of the ground terminals by jointly optimizing the trajectories of the UAVs, the uplink power control, and the time resource allocation for wireless energy transfer and wireless information transmission. The authors in [30] formulated the minimum average rate maximization problem by jointly optimizing the trajectory, velocity, and acceleration of the UAV and the uplink transmit power of ground nodes. In [31], the authors considered the multipoint-to-multipoint UAV enabled wireless networks and aimed to maximize the minimum throughput subject to constraints on multiuser communication scheduling, UAV trajectory and power control.

These results have presented insightful results for coverage optimization. However, they may not be suitable for the IoT communication system. Considering the constraint on size and energy, coverage optimization problem in the IoT communication system should be rigorously designed so that each IoT could access the IoT network with minimum energy consumption. In addition, these studies in [29-31] have assumed an ideal free-space model, which is usually not reasonable and cannot be used to model the link between the mobile UAV and the randomly-scattered IoT devices. To be practical, the UAV should be appropriately placed with a typical channel model. Furthermore, these results [29-31] have assumed the full channel state information (CSI) condition, which is impossible for some mobile UAV-enabled IoT scenarios due to the difficulty in perfectly acquiring the random small-scale channel fading [32,33].

Motivated by the above observations, in this work, we focus on the coverage optimization for a practical UAV-aided IoT communication system. We maximize the minimum average rate of all the IoT devices, by jointly optimizing the partition ratio of the time resource blocks and the UAV altitude. We consider the composite channel model, which consists of both the small-scale and the large-scale channel fading, to practically depict the typical propagation environment. In general, it is difficult to perfectly acquire the random small-scale channel fading. Thus, we use only the large-scale CSI because it is slowly-varying and can be achieved with quite low cost. This framework has been proposed in our previous work [34]. But therein we mainly considered to improve the system efficiency by maximizing the sum rate. In this work, we take a step further to consider coverage optimization of the UAV-aided IoT communications using only the large-scale CSI.

The rest of the paper is organized as follows. Section II presents the general UAV-aided IoT communication system model. Section III formulates the optimization problem to maximize the minimum average rate of the IoT devices, and proposes an efficient iterative algorithm. In Section IV, simulation results are presented. Finally, conclusion is made in Section V. Throughout the paper, $\|\cdot\|$ and $|\cdot|$ denote the Euclidean norm and the absolute value of a complex-valued scalar, respectively.

2 System Model

As shown in Figure 1, we consider a mobile UAV-aided IoT communication system in which K $(K>1)$ IoT devices equipped with single antenna are supported by one single-antenna UAV which serves as a BS. In this system, UAV collects data from the IoT devices for connecting the server. Thus, we focus on the uplink communication from the IoT devices to the UAV. The downlink can be studied in a similar way from the UAV to the IoT devices. All the devices are located with a horizontal distance $r_i,\ i=1,\ldots,K$ to the UAV and an angle $\theta_i,\forall i$ with respect to the UAV. In addition, all the IoT devices are arbitrarily distributed in the cell with a radius r_c $(r_c \geq \max\{r_1,r_2,\ldots r_K\})$. Here, it is assumed that the cell locates at the center (0,0,0), and the coordinate for the IoT device i can be represented as $(r_i\cos(\theta_i),r_i\sin(\theta_i),0)$, where θ_i is the corresponding angle for the device i.

In this system, we assume the UAV locates at an altitude h and flies around the IoT devices following a circular trajectory of radius r_U in a cycling period T_U. That is, UAV could periodically receive the signal from all the IoT devices during the flight. Thus, we have $T_U=\frac{2\pi r_U}{v}$, where v is the velocity of the UAV. Within this circular trajectory, we as-

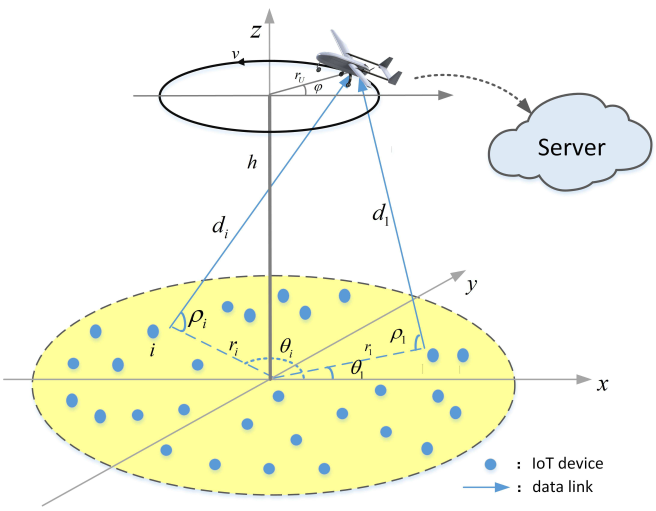

Figure 1 Illustration of a UAV-aided IoT communication system

sume the coordinate $(r_U cos(\varphi), r_U sin(\varphi), h)$ as the UAV initial location, where φ is the corresponding initial phase parameter. Therefore, at the time constant t $(0 \le t \le T_U)$, the time-varying trajectory for the UAV can be denoted as $(r_U \cos(\frac{v}{r_U}t + \varphi), r_U \sin(\frac{v}{r_U}t + \varphi), h)$. In this case, the time-varying distance between IoT device i and the mobile UAV is:

$$d_i(t) = \sqrt{h^2 + r_i^2 + r_U^2 - 2r_i r_U \cos\left(\frac{v}{r_U}t + \varphi - \theta_i\right)}, \quad (1)$$

where θ_i is the corresponding phase for IoT device i.

Similarly, the path loss between the mobile UAV and IoT device i is [19]:

$$PL_i^{dB}(t) = \frac{A}{1 + ae^{-b(\bar{\rho}_i(t) - a)}} + B_i(t), \quad (2)$$

where f is the carrier frequency, c is the speed of light, η_{LOS}, η_{NLOS}, a and b are constants related to the propagation environment,

$$A = \eta_{LOS} - \eta_{NLOS},$$

$$B_i(t) = 20\lg(d_i(t)) + 20\lg(\frac{4\pi f}{c}) + \eta_{NLOS},$$

and

$$\bar{\rho}_i(t) = \frac{180}{\pi} \arcsin\left(\frac{h}{\sqrt{h^2 + r_i^2 + r_U^2 - 2r_i r_U \cos(\frac{v}{r_U}t + \varphi - \theta_i)}}\right)$$

is the elevation angle of the mobile UAV relative to the IoT device i.

Consequently, the absolute power loss between the mobile UAV and the IoT device i can be expressed as:

$$Q_i(t) = 10^{\frac{PL_i(t)}{10}}. \quad (3)$$

In this case, the received signal at the mobile UAV transmitted by the IoT device i is

$$y_i(t) = \sqrt{\frac{p_i}{Q_i(t)}} g_i(t) x_i + z_m, \quad (4)$$

where p_i represents the transmission power used by the IoT device i to transmit data, $g_i(t)$ is the small-scale fading coefficient following the Gaussian distribution according to $\mathscr{CN}(0,1)$, z_m is the additive white Gaussian noise (AWGN) at the mobile UAV and $\delta^2 = E\{|z_m|^2\}$ is the noise variance. Note that in this work, we assume p_i, $\forall i$ are constant when the IoT devices transmit data to the UAV.

In this work, we assume all the IoT devices share the same frequency band for their communications with the UAV over a consecutive duration $T > 0$ in second(s). During this time, all the IoT devices operate via a periodic/cyclical time-division multiple access (TDMA). Here, we assume $T = T_U$ for simplicity.

Note that, the continuous time variables significantly increase the difficulty for mobile UAV. For ease of exposition, we discretize the cyclical flying time T into N time slots, i.e., $T = N\Delta t$ in [20], with Δt representing the length of the unit time slot, which is sufficiently small so that within each time slot, the distance between the mobile UAV and the IoT devices is considered as approximately unchanged whereas the small scale channel fading is time-varying. Furthermore, we assume it consists of amount of time resource blocks in each time slot. Denote $a_i[n]$ as the partition ratio of the time resource blocks for the IoT device i in the time slot n [1]. In this case, we have $0 \le a_i[n] \le 1, \forall i$.

Without loss of generality, we also specify the following constraint

$$\sum_{i=1}^{K} a_i[n] \le 1, \text{ for } i \in 1, ..., K \quad (5)$$

in each time slot.

In the time slot n, the received signal at the mobile UAV from the IoT device i is

$$y_i[n] = \sqrt{\frac{p_i}{Q_i[n]}} g_i[n] x_i + z_m, \quad (6)$$

where $Q_i[n] = Q_i(t)|_{t=n}$, and $g_i[n] = g_i(t)|_{t=n}$.

Then, the average achievable rate of the IoT device i within

[1] Here, the assignment $a_i[n], \forall i, n$ is feasible due to the fact that with the limited size and the constrained battery, the signal processing capability of UAV is also limited. Thus, when the IoT devices transmit data to the UAV, we specify the assignment of the time resource blocks in each time slot.

the flight is [31]

$$\bar{r}_i = \frac{1}{N}\sum_{n=1}^{N} a_i[n]\mathbb{E}\left[\log_2\left(1+\frac{p_i|g_i[n]|^2}{Q_i[n]\delta^2}\right)\right], \tag{7}$$

where $\mathbb{E}(\cdot)$ denotes the expectation operator.

3 Coverage Optimization

In this section, we focus on the minimum average rate maximization for each IoT device [2]. Specially, let $\mathbf{A} = \{a_i[n], \forall i\}$. We address the problem by jointly optimizing the partition ratio of the time resource blocks $\mathbf{A}$ and the UAV altitude h for the mobile UAV-aided IoT communication system. The problem can be reformulated as

$$\max_{\mathbf{A},h} \min_{i} \frac{1}{N}\sum_{n=1}^{N} a_i[n]\mathbb{E}\left[\log_2\left(1+\frac{p_i|g_i[n]|^2}{Q_i[n]\delta^2}\right)\right] \tag{8a}$$

$$\text{s.t. } a_i[n] \in [0,1], \forall i \tag{8b}$$

$$\sum_{i=1}^{K} a_i[n] \leq 1, \forall i \tag{8c}$$

$$h > 0. \tag{8d}$$

where (8c) comes from the constraint (5). In fact, the problem is quite intractable due to the complicated objective function with respect to the altitude h. Because of the expectation operator $\mathbb{E}(\cdot)$, the objective function presents the form of integrals and is difficult to be expressed in a closed form in terms of h. Therefore, problem (9) is challenging to solve with the non-closed-form expression of the achievable average rate $\bar{r}_i$ with respect to h.

Before the further derivation, we define $\kappa(\mathbf{A},h) = \min_{i=1,\dots,K} \bar{r}_i$ as the minimum average rate for simplicity. In this case, the optimization problem can be recast into

$$\max_{\mathbf{A},h,\kappa} \kappa \tag{9a}$$

$$\text{s.t. } \frac{1}{N}\sum_{n=1}^{N} a_i[n]\mathbb{E}\left[\log_2\left(1+\frac{p_i|g_i[n]|^2}{Q_i[n]\delta^2}\right)\right] \geq \kappa, \forall i \tag{9b}$$

$$a_i[n] \in [0,1], \forall i \tag{9c}$$

$$\sum_{i=1}^{K} a_i[n] \leq 1, \forall i \tag{9d}$$

$$h > 0. \tag{9e}$$

In the following, we first derive the closed form of the achievable rate $\bar{r}_i$ in (7) so as to remove the expectation operator $\mathbb{E}(\cdot)$, and then propose an efficient iterative algorithm for the problem.

[2] Note that in this work, we consider the coverage optimization by maximizing the minimum average rate for all the IoT devices. That's because the minimum average rate maximization can achieve the fairness for all the IoT devices.

3.1 The closed form of the achievable average rate $\bar{r}_i$

Based on the remarkable studies [35,36], we introduce the closed form of the achievable average rate $\bar{r}_i$ by applying the random theory matrix as

$$\begin{aligned}\bar{r}_i^{ap} = \frac{1}{N}\sum_{n=1}^{N} a_i[n]\Bigg\{ &\log_2\left(1+\frac{p_i}{\mu_{i,n}Q_i[n]\delta^2}\right) \\ &+\log_2 e\left[\ln(\mu_{i,n}) - 1 + \frac{1}{\mu_{i,n}}\right]\Bigg\}, \forall i,\end{aligned} \tag{10}$$

where $\mu_{i,n}, i = 1,\dots,K$ can be uniquely defined as the following fixed-point equation

$$\mu_{i,n} = 1 + \frac{p_i}{Q_i[n]}\left(\delta^2 + \frac{p_i}{\mu_{i,n}Q_i[n]}\right)^{-1}, \forall i,n. \tag{11}$$

Based on [35], it is easy to know the performance gap between $\bar{r}_i$ and $\bar{r}_i^{ap}$ can be negligible. Thus, the above approximation is quite accurate.

In IoT communication system, most IoT devices generally have the limited energy. However, in some complex communication environment, e.g., downtown, urban and rural areas, there exists a large amount of noise sources, which significantly influence the signal transmitted by the IoT devices. Thus, IoT communication system usually has low SNR. In this case, the fixed-point equation $\mu_{i,n}$ can be further approximated as

$$\begin{aligned}\mu_{i,n} &= 1 + \frac{p_i}{Q_i[n]}\left(\delta^2 + \frac{p_i}{\mu_{i,n}Q_i[n]}\right)^{-1} \\ &\overset{(a)}{\approx} 1 + \frac{p_i}{Q_i[n]\delta^2} \\ &\overset{(b)}{\approx} 1, \forall i,n.\end{aligned} \tag{12}$$

where (a) holds due to the fact that with low SNR assumption, it follows $\delta^2 \gg \frac{p_i}{\mu_{i,n}Q_i[n]}$. (b) holds due to the fact that $\frac{p_i}{Q_i[n]\delta^2}$ approaches 0 based on the low SNR assumption. As a result, we have

$$\bar{r}_i^{ap} = \frac{1}{N}\sum_{n=1}^{N} a_i[n]\left[\log_2\left(1+\frac{p_i}{Q_i[n]\delta^2}\right)\right], \forall i. \tag{13}$$

3.2 An iterative algorithm for the minimum average rate maximization

Based on the closed form of the achievable average rate $\bar{r}_i$ derived in subsection 3.1, problem (9) can be further reformu-

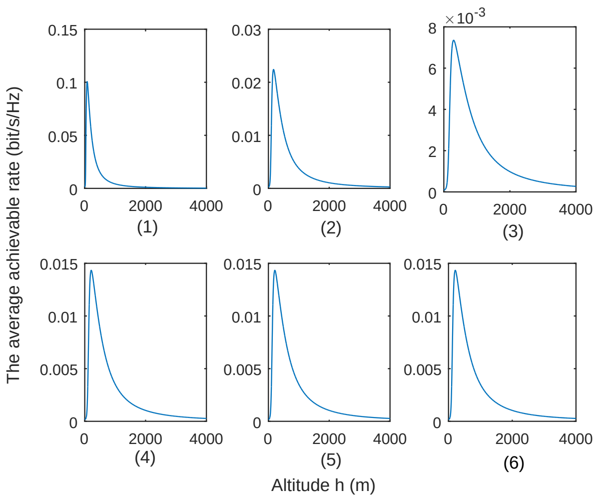

Figure 2 Illustration of the non-convexity of $\bar{r}_i^{ap}$ in terms of h based on the simulation setting in Section 4, where we consider $K = 6$ IoT devices and assume $v = 2$m/s, $\delta^2 = -65$dBm, $T = 200$s, $p_i = 0.01$W, $\forall i$.

lated into

$$\max_{\mathbf{A},h,\kappa} \ \kappa \tag{14a}$$

$$\text{s.t.} \ \frac{1}{N}\sum_{n=1}^{N} a_i[n]\left[\log_2\left(1+\frac{p_i}{Q_i[n]\delta^2}\right)\right] \geq \kappa, \forall i \tag{14b}$$

$$a_i[n] \in [0,1], \forall i,n \tag{14c}$$

$$\sum_{i=1}^{K} a_i[n] \leq 1, \forall n \tag{14d}$$

$$h > 0. \tag{14e}$$

Since the constraint (14b) is not convex with respect to h as illustrated in Figure 2, problem (14) is not convex. In the following, to tackle the non-convex difficulty we propose an effective scheme for the non-convex problem (14) by using the block coordinate descent [37], in which the partition ratio of the time resource blocks $\mathbf{A}$ and the altitude h are alternately optimized in each iteration.

1) The optimization of the partition ratio of the time resource blocks $\mathbf{A}$

For any given altitude h, the optimization of the partition ratio of the time resource blocks $\mathbf{A}$ can be recast into

$$\max_{\mathbf{A},\kappa} \ \kappa \tag{15a}$$

$$\text{s.t.} \ (14\text{b}), (14\text{c}), (14\text{d}). \tag{15b}$$

Problem (15) is convex, which can be solved by the toolbox CVX.

2) The optimization of the altitude h

For any given partition ratio of the time resource blocks $\mathbf{A}$, the optimization of the altitude h can be rewritten as

$$\max_{h,\kappa} \ \kappa \tag{16a}$$

$$\text{s.t.} \ \frac{1}{N}\sum_{n=1}^{N} a_i[n]\log_2\left(1+\frac{p_i}{Q_i[n]\delta^2}\right) \geq \kappa, \forall i \tag{16b}$$

$$h > 0. \tag{16c}$$

Note that problem (16) is neither a convex nor concave problem due to the non-convex constraint (16b), which can be depicted in Figure 2. In general, there is no efficient method to obtain the optimal solution.

To handle the non-convexity of the constraint (16b), we adopt the successive convex optimization technique, in which the original optimization function can be approximated in a tractable one at a given local point in each iteration. Let $h^{(q)}$ be the local point of h at the q-th iteration in the successive convex optimization technique. Then, $\bar{r}_i^{ap}$ can be lower-bounded by its first-order Taylor expansion around the point $h^{(q)}$.

For the IoT device i, since the absolute power loss at the n-th time slot $Q_i[n]$ is related to the elevation angle of the mobile UAV relative to the IoT device i and the distance between them, it is quite complicated. To facilitate the first-order derivation of $\bar{r}_i^{ap}$ at the local point $h^{(q)}$, we first consider the first-order derivation of $Q_i[n]$ at the local point $h^{(q)}$. Here, we set

$$Q_i[n] = 10^{\frac{F_i[n]+B_i[n]}{10}}, \tag{17}$$

where

$$F_i[n] = \frac{A}{1+ae^{-b(\bar{\rho}_i[n]-a)}},$$

$$B_i[n] = 20\lg(d_i[n]) + 20\lg(\frac{4\pi f}{c}) + \eta_{NLOS},$$

$$\bar{\rho}_i[n] = \frac{180}{\pi}\arcsin\left(\frac{h}{\sqrt{h^2+r_i^2+r_U^2-2r_ir_U\cos(\frac{v}{r_U}n+\varphi-\theta_i)}}\right),$$

and

$$d_i[n] = \sqrt{h^2+r_i^2+r_U^2-2r_ir_U\cos\left(\frac{v}{r_U}n+\varphi-\theta_i\right)}.$$

The first-order derivation of $F_i[n]$ at the local point $h^{(q)}$ is

$$F_{i,q}[n] = \frac{180Abae^{-bC_{i,q}[n]}}{\pi\left(D_{i,q}[n]\right)^2\sqrt{1-\left(\frac{h^{(q)}}{d_{i,q}[n]}\right)^2}}\left[\frac{1}{d_{i,q}[n]} - \frac{(h^{(q)})^2}{(d_{i,q}[n])^3}\right], \tag{18}$$

where

$$d_{i,q}[n]=\sqrt{(h^{(q)})^2+r_i^2+r_U^2-2r_ir_U\cos(\frac{v}{r_U}n+\varphi-\theta_i)},$$
$$C_{i,q}[n]=\frac{180}{\pi}\arcsin\frac{h^{(q)}}{d_{i,q}[n]}-a,$$
$$D_{i,q}[n]=1+ae^{-bC_{i,q}[n]}.$$

The first-order of $B_i[n]$ at the local point $h^{(q)}$ is

$$B_{i,q}[n]=\frac{20h^{(q)}}{(d_{i,q}[n])^2}\lg e. \tag{19}$$

By taking the first-order Taylor expansion at the local point $h^{(q)}$, $\bar{r}_i^{ap}$ can be lower-bounded by

$$\begin{aligned}\bar{r}_i^{ap}&\geq\bar{r}_i^{aplb}\\&=\frac{1}{N}\sum_{n=1}^{N}a_i[n]\log_2\left(1+\frac{p_i}{Q_i^q[n]\delta^2}\right)\\&-\frac{\log_2 10}{10}\frac{1}{N}\sum_{n=1}^{N}a_i[n]\frac{p_i(F_{i,q}[n]+B_{i,q}[n])}{p_i+Q_i^q[n]\delta^2}(h-h^{(q)}),\end{aligned} \tag{20}$$

where $Q_i^q[n]=10^{\frac{F_i^q[n]+B_i^q[n]}{10}}$, $F_i^q[n]=F_i[n]|_{h=h^{(q)}}$ and $B_i^q[n]=B_i[n]|_{h=h^{(q)}}$.

Thus, with the local point $h^{(q)}$ and the lower bound $\bar{r}_i^{aplb}$ in (20), problem (16) can be further recast into

$$\max_{h,\kappa}\ \kappa_{aplb} \tag{21a}$$
$$\text{s.t. } \bar{r}_i^{aplb}\geq\kappa,\forall i, \tag{21b}$$
$$h>0. \tag{21c}$$

where κ_{aplb} is the lower bound of κ.

Now problem (21) is convex, and can be solved by the toolbox CVX. By iteratively optimizing (21) at the given point $h^{(q)}$ which is updated in each iteration, problem (16) can be solved. The details are summarized in Algorithm 1. According to the analysis in [23,24], it is clear that the resulting objective value of problem (21) in Algorithm 1 is non-decreasing in each iteration. Accordingly, Algorithm 1 could be guaranteed to converge.

The overall algorithm for problem (9) can be achieved by alternately solving problem (15) and problem (16) in an iterative manner. The details of the algorithm can be summarized in Algorithm 2.

Next, we analyze the convergence of the proposed Algorithm 2. It is pointing out that to achieve the optimal altitude h, problem (16) is solved through its approximate problem (21) based on Algorithm 1. Thus, we cannot directly apply the general convergence analysis that is for the classical block coordinate descent method [24,31]. In the classical block coordinate descent method, each optimization problem in each block should be strictly solved with its exact optimality in each iteration [37]. Thus, we make a further convergence analysis for our proposed scheme.

Algorithm 1 The proposed algorithm for solving problem (16)

1: **Initialize**: the UAV altitude $h^{(0)}$ and the accuracy $\varepsilon>0$. Set $q=0$.
2: **repeat**
3: Solve problem (21) for given $h^{(q)}$ to obtain the optimal solution $h^{(q+1)}$.
4: $h^{(q)}\leftarrow h^{(q+1)}$; $q\leftarrow q+1$.
5: **until** The fractional increase of the objective function is below the threshold $\varepsilon>0$.

Based on problem (15), problem (16) and its approximate problem (21), we have

$$\begin{aligned}\kappa(\mathbf{A}^{(k)},h^{(k)})&\overset{(a)}{\leq}\kappa\left(\mathbf{A}^{(k+1)},h^{(k)}\right)\\&\overset{(b)}{=}\kappa_{aplb}\left(\mathbf{A}^{(k+1)},h^{(k)}\right)\\&\overset{(c)}{\leq}\kappa_{aplb}\left(\mathbf{A}^{(k+1)},h^{(k+1)}\right)\\&\overset{(d)}{\leq}\kappa\left(\mathbf{A}^{(k+1)},h^{(k+1)}\right)\end{aligned} \tag{22}$$

where $\kappa(\mathbf{A},h)$ has been defined prior to problem (9). (a) holds due to the optimal solutions of problem (15) with the given altitude $h^{(k)}$; (b) holds due to the convergence of Algorithm 1; (c) holds since $\left(h^{(k+1)},\kappa_{aplb}^{(k+1)}\right)$ is the optimal solution of problem (21) with the given $\mathbf{A}^{(k+1)}$, and (d) holds since the objective value of problem (21) is the lower bound of that of problem (16) at $h^{(k+1)}$ with the given $\mathbf{A}^{(k+1)}$. The result in (22) indicates that the objective value of problem (14) is non-decreasing in each iteration of Algorithm 2. Thus, the proposed Algorithm 2 can be guaranteed to converge.

Algorithm 2 The proposed algorithm for solving problem (9)

1: **Initialize**: the UAV altitude $h^{(0)}$ and the accuracy $\bar{\varepsilon}>0$. Let $k=0$.
2: **repeat**
3: Solve problem (15) for given $h^{(k)}$ to obtain the optimal $\mathbf{A}^{(k+1)}$.
4: Solve problem (16) for given $\mathbf{A}^{(k+1)}$ and $h^{(k)}$ using Algorithm 1 to obtain the optimal $h^{(k+1)}$.
5: $k\leftarrow k+1$.
6: **until** The fractional increase of the objective function is below the threshold $\bar{\varepsilon}$.

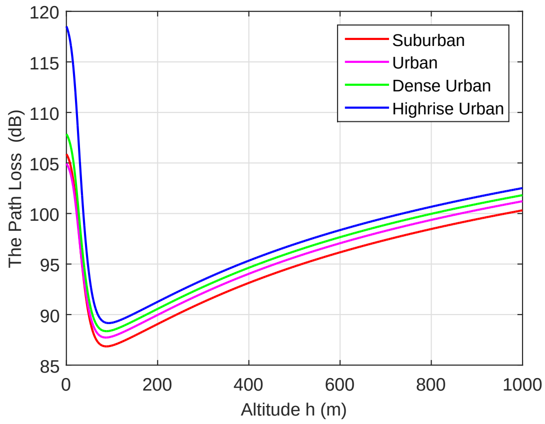

Figure 3 The path loss (dB) versus different altitude h in the different propagation environment for one IoT device

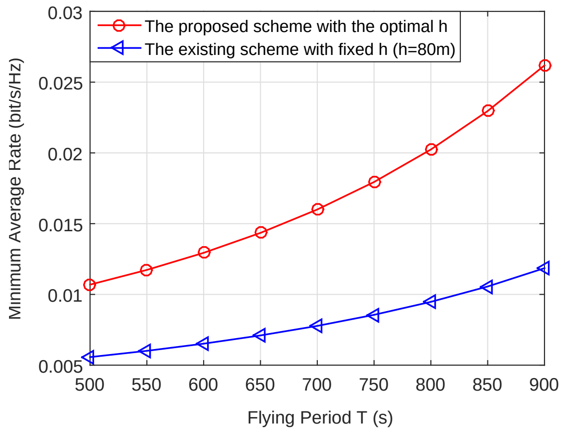

Figure 4 The minimum average rate versus different flying periods

4 Numerical Results and Discussion

In this section, we verify the effectiveness of our proposed scheme by means of simulation [3]. We set the frequency $f = 2.4$GHz, the speed of light $c = 3\times10^8$m/s and the corresponding initial phase parameter $\varphi = \frac{\pi}{6}$. For the system, we assume six ($K = 6$) IoT devices, which are uniformly distributed within a cell [4]. In addition, we assume the random realizations of the IoT devices are located with horizontal distances $r_1 = 189$m, $r_2 = 260$m, $r_3 = 298$m, $r_4 = 450$m, $r_5 = 680$m and $r_6 = 759$m. We also set $\theta_1 = \frac{\pi}{6}$, $\theta_2 = \frac{\pi}{3}$, $\theta_3 = \frac{2}{3}\pi$, $\theta_4 = \frac{5}{6}\pi$,$\theta_5 = \frac{3}{2}\pi$, $\theta_6 = \frac{10}{9}\pi$. The thresholds presented in Algorithm 1 and 2 are fixed as $\varepsilon = \bar{\varepsilon} = 10^{-4}$. The initial value $h^{(0)}$ in Algorithm 1 is 100m. Also, we consider the typical propagation environment using the following $(\eta_{LoS}, \eta_{NLoS})$ pairs $(0.1, 21)$, $(1.0, 20)$, $(1.6, 23)$, $(2.3, 34)$ corresponding to suburban, urban, dense urban, and highrise urban, respectively.

Figure 3 presents the path loss versus the UAV altitude h in different propagation environment. We choose any one IoT device, i.e., $r_1 = 189$m and $\theta_1 = \frac{\pi}{6}$. The curves are achieved based on the equation $\frac{1}{N}\sum_{n=1}^{N} PL_i^{dB}(n)$ during the UAV's flight, where $i = 1$. Here, we set $T = 100s$. It can be seen that the path loss first reduces quickly as the altitude h increases. Once it achieves the lowest point, it increases when the altitude h becomes high. Obviously, there must exist an optimal h that makes the absolute power loss achieve the lowest point. In this case, the system has the best performance. In addition, it can be also seen that the path loss has a high dependence on the practical propagation environment.

In order to show the performance of Algorithm 2 in our proposed scheme, in Figure 4, we compare the minimum average rate achieved by the proposed scheme using the optimal h with that obtained by the conventional scheme using a fixed h [31] in the suburban environment, where we assume the noise variance $\delta^2 = -80$dBm,, the transmission power of all the IoT devices $p_i = 0.05$W, $\forall i$, the UAV constant speed $v = 2$m/s and the initial value $h^{(0)} = 100$m in Algorithm 2. It can be seen the minimum average rate achieved by Algorithm 2 significantly outperforms that with the fixed h. That's because by optimizing the altitude h, the mobile UAV could locate a best altitude to adapt the communication with the randomly-scattered IoT devices during its flying period. In this case, there has the lowest path loss (as illustrated in Figure 3) between the UAV and the IoT devices. Thus, IoT devices could achieve the best average rate. In contrast, fixing the UAV's altitude would restrict the potential of the UAV's mobility. Accordingly, it is impossible to achieve the optimal altitude for the mobile UAV.

Figure 5 presents the minimum average rate obtained by Algorithm 2 in different urban scenarios. Here, we assume that $\delta^2 = -80$dBm, $v = 2$m/s, $p_i = 0.01$W, $\forall i$ and specify the initial value $h^{(0)}$ in Algorithm 2 is 80m. It can be observed, in the different propagation environment, the achievable minimum average rate presents the various behavior. That comes from that the optimal h is highly dependent on the practical urban environment, which could result in the difference of the minimum average rate when we derive the average rate by our proposed scheme. In addition, it can also be seen that as the flying period T becomes large, the minimum average rate increases. The largest minimum average rate is achieved in the urban area, and the smallest minimum average rate is obtained in the highrise urban area.

Figure 6 illustrates the comparison between the minimum average rate obtained by our proposed scheme with optimal h and that obtained by the existing scheme with the fixed h [31] in terms of different transmission powers. We assume $\delta^2 = -80$dBm, $T = 700$s and $v = 2$m/s. We also set the ini-

[3] The simulation is based on the low SNR assumption.

[4] For simplicity, we assume $K = 6$ IoT devices in this simulation. However, the proposed algorithms is also applicable for the cases where there exists a large amount of IoT devices.

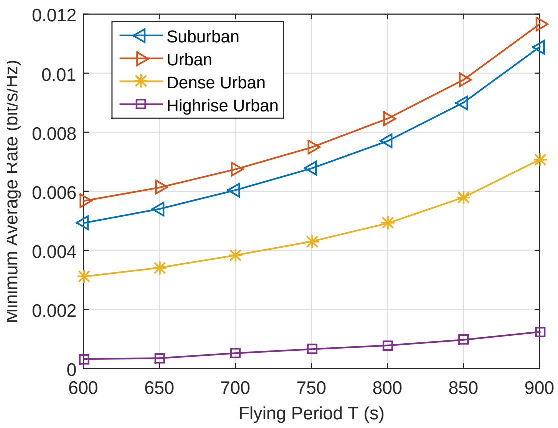

Figure 5 The minimum average rate versus different flying periods in the different urban environment

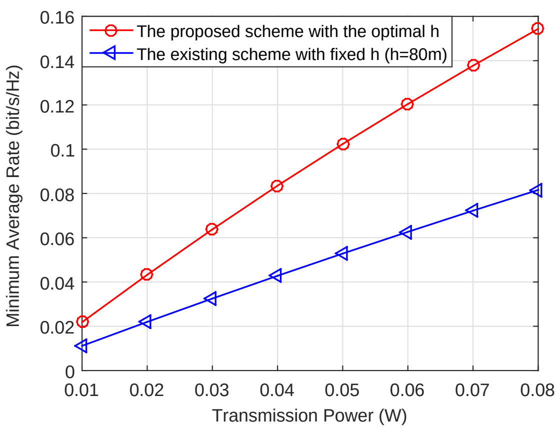

Figure 6 The minimum average rate versus different transmission powers

tial value $h^{(0)}$ in Algorithm 2 is 100m. Here, we consider the suburban environment. It is easy to see that the minimum average rate obtained by Algorithm 2 is larger than that obtained by the existing scheme. With the optimization of UAV altitude, UAV could adaptively choose the best placement to communicate with the IoT devices. In this case, the absolute power loss achieves the lowest, and the average minimum rate is largest. In addition, the minimum average rate increases as the transmission power increases. That is due to the fact that the achievable rate of all the IoT devices within the flight increases linearly with the transmission power.

5 Conclusion

In this paper, we investigated the UAV-aided IoT communications system, and considered the coverage optimization problem for this system with partial channel knowledge. Specially, we maximized the minimum average rate by jointly optimizing the partition ratio of the time resource blocks and the UAV altitude. To characterize the practical propagation environment, the composite channel model including both the small-scale and the large-scale channel fading was adopted. Full CSI assumption was not available because it was impossible to acquire the time-varying small-scale channel fading in practice. We only used the slowly-varying large-scale channel fading. The formulated problem was not convex. An efficient iterative algorithm was proposed by means of the block coordinate descent and the successive convex optimization technique. Numerical results have demonstrated that the performance with the altitude optimization significantly outperformed that with the fixed altitude. Furthermore, the results also implied that the performance of the UAV-aided IoT communications system was strongly dependent on the specific urban environment.

6 Acknowledgment

This work was supported in part by Beijing Natural science Foundation under grant No. L172041, and the National Science Foundation of China under grant No. 61701457, grant No. 61771286, grant No. 91638205, grant No. 61671478 and grant No. 61621091.

References

[1] L. D. Xu, W. He, S. Li. Internet of Things in industries: A survey [J]. IEEE Transaction on Industrial Informatics, 2014, 10(4): 2233-2243.

[2] C. Zhu, J. J. P. C. Rodrigues, V. C. M. Leung, et al. Trust-based communication for the industrial Internet of Things [J]. IEEE Commununications Magazine, 2018, 56(2): 16-22.

[3] L. Hou, S. Zhao, X. Xiong, et al. Internet of Things Cloud: Architecture and Implementation [J]. IEEE Commununications Magazine, 2016, 54(12): 32-39.

[4] I. Bisio, F. Lavagetto, G. Luzzati. Cooperative Application Layer Joint Video Coding in the Internet of Remote Things [J]. IEEE Internet of Things Journal, 2016, 3(6): 1418-1426.

[5] D. Pal, S. Funilkul, N. Charoenkitkarn, et al. Internet-of-Things and Smart Homes for Elderly Healthcare: An End User Perspective [J]. IEEE Access, 2018, 6: 10483-10496.

[6] J. Delsing. Local cloud Internet of Things automation: Technology and business model features of distributed In-

ternet of Things automation solutions [J]. IEEE Industrial Electronics Magazine, 2017, 11(4): 8-21.

[7] V. Sharma, R. Kumar, R. Kaur. UAV-assisted content-based sensor search in IoTs [J]. Electronics Letter, 2017, 53(11): 724-726.

[8] S. Lien, K. Chen, Y. Lin. Toward ubiquitous massive accesses in 3GPP machine-to-machine communications [J]. IEEE Communications Magazine, 2011, 49(4): 66-74.

[9] V. Scilimati, A. Petitti, P. Boccadoro, et al. Industrial Internet of things at work: a case study analysis in robotic-aided environmental monitoring [J]. IET Wireless Sensor Systems, 2017, 7(5): 155-162.

[10] N. H. Motlagh, M. Bagaa, T. Taleb. UAV-based iot platform: A crowd surveillance use case [J]. IEEE Communications Magazine, 2017, 55(2): 128-134.

[11] N. Hossein Motlagh, T. Taleb, O. Arouk. Low-Altitude Unmanned Aerial Vehicles-Based Internet of Things Services: Comprehensive Survey and Future Perspectives [J]. IEEE Internet of Things Journal, 2016, 3(6): 899-922.

[12] M. Gharibi, R. Boutaba, S. L. Waslander. Internet of Drones [J]. IEEE Access, 2016, 4: 1148-1162.

[13] Q. Yang, S. Yoo. Optimal UAV Path Planning: Sensing Data Acquisition Over IoT Sensor Networks Using Multi-Objective Bio-Inspired Algorithms [J]. IEEE Access, 2018, 6: 13671-13684.

[14] A. Giyenko, Y. I. Cho. Intelligent UAV in smart cities using IoT [C]//2016 16th International Conference on Control, Automation and Systems, Gyeongju, 2016: 207-210.

[15] G. Ding, Q. Wu, L. Zhang, et al. An Amateur Drone Surveillance System Based on the Cognitive Internet of Things [J]. IEEE Communications Maganize, 2018, 56(1): 29-35.

[16] S. Arabi, H. Elbiaze, E. Sabir, et al. Tradeoffs for Data Collection and Wireless Energy Transfer Dilemma in IoT Environments [C]//2018 IEEE International Conference on Communications, Kansas City, MO, 2018: 1-6.

[17] D. He, S. Chan, M. Guizani. Communication security of unmanned aerial vehicles [J]. IEEE Wireless Communications, 2017, 24(4): 134-139.

[18] S. Chandrasekharan, K. Gomez, A. Al-Hourani, et al. Designing and implementing future aerial communication networks [J]. IEEE Communications Maganize, 2016, 54(5): 26-34.

[19] A. Al-Hourani, S. Kandeepan, S. Lardner. Optimal LAP Altitude for Maximum Coverage [J]. IEEE Wireless Communications Letter, 2014, 3(6): 569-572.

[20] Y. Zeng, R. Zhang, T. J. Lim. Throughput maximization for UAV-enabled mobile relaying systems [J]. IEEE Transaction on Communications, 2016, 64(12): 4983-4996.

[21] F. Jiang, A. L. Swindlehurst. Optimization of UAV heading for the ground-to-air uplink [J]. IEEE Journal on Selected Areas in Communications, 2012, 30(5): 993-1005.

[22] M. M. Azari, F. Rosas, K. Chen, et al. Joint Sum-Rate and Power Gain Analysis of an Aerial Base Station [C]//2016 IEEE Globecom Workshops, Washington, DC, 2016: 1-6.

[23] Y. Zeng, R. Zhang. Energy-efficient UAV communication with trajectory optimization [J]. IEEE Transaction on Wireless Communications, 2017, 16(6): 3747-3760.

[24] C. Zhan, Y. Zeng, R. Zhang. Energy-Efficient Data Collection in UAV Enabled Wireless Sensor Network [J]. IEEE Wireless Communications Letter, 2018, 7(3): 328-331.

[25] F. Ono, H. Ochiai, R. Miura. A Wireless Relay Network Based on Unmanned Aircraft System With Rate Optimization[J]. IEEE Transaction on Wireless Communications, 2016, 15(11): 7699-7708.

[26] M. M. Azari, F. Rosas, K. Chen, et al. Ultra Reliable UAV Communication Using Altitude and Cooperation Diversity[J]. IEEE Transactions on Communications, 2018, 66(1): 330-344.

[27] T. Qi, W. Feng, Y. Wang. Outage performance of non-orthogonal multiple access based unmanned aerial vehicles satellite networks [J]. China Communications, 2018, 15(5): 1-8.

[28] Y. Chen, W. Feng, G. Zheng. Optimum placement of UAV as relays [J]. IEEE Communications Letters, 2018 22(2): 248-251.

[29] J. Park, H. Lee, S. Eom, et al. Minimum Throughput Maximization in UAV-Aided Wireless Powered Communication Networks [J]. arXiv preprint arXiv:1801.02781, 2018.

[30] S. Eom, H. Lee, J. Park, et al. UAV-Aided Wireless Communication Designs With Propulsion Energy Limitations [J]. arXiv preprint arXiv:1801.02782, 2018.

[31] Q. Wu, Y. Zeng, R. Zhang. Joint Trajectory and Communication Design for Multi-UAV Enabled Wireless Networks [J]. IEEE Transaction on Wireless Communications, 2018, 17(3): 2109-2121.

[32] C. Liu, W. Feng, T. Wei, et al. Fairness-oriented hybrid precoding for massive MIMO maritime downlink systems with large-scale CSIT [J]. China Communications, 2018, 15(1): 52-61.

[33] W. Feng, Y. Wang, D. Lin, et al. When mmWave communications meet network densification: a scalable interference coordination perspective [J]. IEEE Journal on Selected Areas in Communications, 2017, 35(7): 1459-1471.

[34] W. Feng, J. Wang, Y. Chen, et al. UAV-Aided MIMO communications for 5G Internet of Things [J]. IEEE Internet of Things Journal, to appear, 2018.

[35] W. Feng, Y. Wang, N. Ge, et al. Virtual MIMO in Multi-Cell Distributed Antenna Systems: Coordinated Transmissions with Large-Scale CSIT [J]. IEEE Journal on Selected Areas Communications, 2013, 31(10): 2067-2081.

[36] W. Feng, N. Ge, J. Lu. Coordinated satellite-terrestrial networks: a robust spectrum sharing perspective [C]//2017 26th Wireless and Optical Communication Conference, Newark, New Jersey, USA, 2017: 1-5.

[37] D. P. Bertsekas. Nonlinear programming [M]. Athena scientific Belmont, 1999.

About the authors

Xuanxuan Wang received the B.S. degree in communication engineering from Henan Polytechnic University, in 2010, and the M.S. degree in electronic and communication engineering from Beijing University of Posts and Telecommunications, Beijing, China, in 2013. She received the Ph.D. degree from Institute of Information and Engineering, Chinese Academy of Sciences, China, in 2017. She is with the Department of Electronic Engineering, Tsinghua University. Her current research interests include communication security, wireless information and power transfer, and convex optimization techniques. (wangxuanuxuan@tsinghua.edu.cn)

Wei Feng (S'06-M'10), corresponding author, received his B.S. and Ph.D. degrees (both with the highest honor) from the Department of Electronic Engineering, Tsinghua University, Beijing, China, in 2005 and 2010, respectively. From 2010 to 2011, he served as a Project Director in the National Science and Technology Major Project Management Office of Tsinghua University. From 2011 to 2014, he was a Postdoctoral Research Fellow with the Department of Electronic Engineering, Tsinghua University, where he has been an Assistant Professor since Oct. 2014 and then an Associate Professor since Dec. 2016. His research interests include maritime broadband communication networks, large-scale distributed antenna systems, and coordinated satellite-terrestrial networks. He has published over 70 journal and conference papers. He also holds over 10 granted patents. Dr. Feng has received the Outstanding Ph.D. Graduate of Tsinghua University Award in 2010, the IEEE WCSP Best Paper Award in 2013, the first Prize of Science and Technology Award of China Institute of Communications in 2015, the IEEE WCSP Best Paper Award in 2015, and the second Prize of National Technological Invention Award of China in 2016. He currently serves as the Assistant to the Editor-in-Chief of China Communications. (fengwei@tsinghua.edu.cn)

Yunfei Chen (S'02-M'06-SM'10) received his B.E. and M.E. degrees in Electronic Engineering from Shanghai Jiao Tong University, China, in 1998 and 2001, respectively. He received his Ph.D. degree from the University of Alberta, Canada, in 2006. He is with the School of Engineering, Warwick University, Coventry, UK. His research interests include energy harvesting, wireless relaying and general performance analysis and design of wireless systems. (Yunfei.Chen@warwick.ac.uk)

Ning Ge (M'97) received the B.S. and Ph.D. degrees from Tsinghua University, Beijing, China, in 1993 and 1997, respectively. From 1998 to 2000, he was involved in the development of ATM switch fabric ASIC at ADC Telecommunications, Dallas, TX, USA. Since 2000, he has been with the Department of Electronic Engineering, Tsinghua University, where he is currently a Professor and also serves as the Director of the Communication Institute. He has authored over 60 papers. His current interests include the areas of communication ASIC design, short range wireless communication, and wireless communications. Dr. Ge is a Senior Member of CIC and CIE. (gening@tsinghua.edu.cn)